PHOTOPRODUCTION OF MESONS OFF THE DEUTERON*

Bernd Krusche, Igal Jaegle

on behalf of the CBELSA/TAPS Collaboration

Department of Physics, University of Basel, 4056 Basel, Switzerland

(Received February 4, 2008)

Photoproduction of mesons off the deuteron has been measured at a tagged photon beam of the Bonn ELSA electron accelerator with the combined Crystal Barrel–TAPS electromagnetic calorimeter for incident photon energies up to 2.5 GeV. The mesons have been detected in coincidence with recoil protons, neutrons and deuterons. This allows the investigation of meson production reactions off the quasifree nucleons bound in the deuteron, as well as coherent production off the deuteron. The comparison of the quasifree proton data to free proton data can pin down possible nuclear effects on the extracted cross-section data. The comparison of quasifree proton and neutron data is then used for the extraction of the isospin structure of the electromagnetic excitation. The quasifree data have been analyzed for the production of η, η', $\pi^0\pi^0$, and $\pi^0\eta$ mesons. Contributions from coherent production have been observed for $\pi^0\eta$ and $\pi^0\omega$ pairs.

PACS numbers: 13.60.Le, 14.20.Gk, 14.40.Aq, 25.20.Lj

1. Introduction

The motivation for the investigation of the photoproduction of mesons off the deuteron and other light nuclei is twofold: quasifree photoproduction of mesons off the neutron allows to study the electromagnetic excitation spectrum of the neutron and final state interaction processes give access to the meson–nucleon interaction.

The excitation spectrum of the nucleon is far from being understood. In particular, it is still not known if the problem of "missing resonances" (many more states predicted in quark models than observed in experiment) is caused by experimental bias or if baryon models use inapt effective degrees of freedom. Most states have been first observed with hadron induced reactions, in particular elastic scattering of charged pions. It is thus possible that the data base is biased against states that couple only weakly to πN.

* Presented at the Symposium on Meson Physics, Kraków, Poland, October 1–4, 2008.

The large progress in accelerator and detector technology made during the last two decades, now allows to study the electromagnetic excitation of resonances with comparable precision, although the cross-sections are typically smaller by two orders of magnitude. These experiments have developed into two directions: measurements of photon induced meson production reactions up to high excitation energies and for many different nucleon–meson final states with the aim to identify at least some of the "missing" states (see *e.g.* [1]) and precise investigations of the properties of known low lying nucleon resonances (see *e.g.* [2]). Although experimental programs for the study of nucleon resonances off the proton are well developed, so far much less effort has gone into the investigation of the corresponding excitations of the neutron. However, this is the only possibility to disentangle the isospin structure of the electromagnetic resonance excitations. Moreover, in some cases the electromagnetic coupling of resonances to the neutron ground state can be stronger than in the proton case, so that certain resonances potentially can be studied in more detail on the neutron.

The study of the interaction of mesons with nucleons and nuclei has largely contributed to our understanding of the strong force. In the case of long-lived mesons like charged pions or kaons, secondary beams can be prepared, which allow the detailed investigation of such interactions. Much less is known for short-lived mesons. Their interaction with nuclei is only accessible in indirect ways for example when the mesons are first produced in the nucleus from the interaction of some incident beam and then subsequently undergo final state interaction (FSI) in the same nucleus. For this purpose, the coherent photoproduction of mesons, where initial and final state nucleus are identical, is of particular interest since the results can be much more easily interpreted than for more complex final states with nucleons removed from the target nucleus.

A well explored example for both topics — excitations of the neutron and FSI effects — is the photoproduction of η mesons. For the free proton it has been widely used for the investigation of the $S_{11}(1535)$ resonance, which dominates this reaction in the threshold region [3–7] and, more recently, also resonance contributions at higher incident photon energies have been studied [8–12]. The investigation of quasifree and coherent η photoproduction off ^{2}H and ^{3,4}He [13–19] has clarified the isospin structure of the $S_{11}(1535)$ electromagnetic excitation, which was found to be dominantly iso-vector (see [2] for a summary). However, at energies above the $S_{11}(1535)$ models predict a significant rise of the ratio due to the contribution of higher lying resonances. In the work of Chiang *et al.* [20] ("Eta-MAID"), the largest contributions comes from the $D_{15}(1675)$ resonance, which is known to have a strong electromagnetic coupling to the neutron [21]. On the other hand, also in the framework of the chiral soliton model [22] a state is predicted in this energy range, which has stronger photon couplings to the neutron than

to the proton and a large decay branching ratio into $N\eta$. This state is the nucleon-like member of the predicted anti-decuplet of pentaquarks, which would be a P_{11} state. Therefore, it is desirable to extend the data into the region of incident photon energies around 1 GeV, where first results from the GRAAL experiment indeed indicated some structure in the excitation function of the $n(\gamma,\eta)n$ reaction.

Finally, measurements of quasifree photoproduction from heavy nuclei were used to extract the ηN absorption cross-section and to study the in-medium properties of the $S_{11}(1535)$ resonance [24–27]. The interaction of η mesons with nuclei is of particular interest because the existence of bound η-nucleus systems has been discussed. The pion-nucleon interaction at small pion momenta is weak, so that no bound pion-nucleus states can exist. However, the η–N interaction at small momenta is shaped by the existence of the s-wave nucleon resonance $S_{11}(1535)$ close to the η production threshold, which couples strongly to the $N\eta$-channel. The η–N interaction has been investigated via the threshold behavior of hadron induced η production reactions, in particular $pp \to pp\eta$ [28–30], $np \to d\eta$ [31, 32], $pd \to \eta^3\mathrm{He}$ [33], $dp \to \eta^3\mathrm{He}$ [34, 35], $\vec{d}\vec{d} \to \eta^4\mathrm{He}$ [36], and $pd \to pd\eta$ [37]. All reactions show more or less pronounced threshold enhancements. However, so far there is no conclusive evidence that the final state interaction is strong enough to form quasi-bound states. If such states do exist, they should show up as threshold enhancements independently of the initial state of the reaction. Threshold photoproduction of η mesons from light nuclei was also investigated in detail [17, 19] and again, threshold enhancements were observed. The most promising signal so far was found in the $^3\mathrm{He}(\gamma,\eta)^3\mathrm{He}$ reaction, although the statistical significance is still weak.

In this contribution recent final and preliminary results from the quasi-free photoproduction of η and η' mesons as well as $\pi^0\pi^0$ pairs off neutrons bound in the deuteron are summarized. Furthermore, very preliminary results for the coherent photoproduction of $\pi^0\eta$ and $\pi^0\omega$ pairs off the deuteron are discussed. The latter may open up new possibilities for the search for η- (and ω-) mesic nuclei. In comparison to the single η production channel they offer two important advantages. Coherent production of single η mesons is strongly suppressed for most nuclei since the dominating excitation of the S_{11} is iso-vector, so that neutron and proton amplitudes cancel to a large extent. However, the $\eta\pi^0$ final state is dominantly populated by a sequential $\gamma N \to \Delta^\star \to \eta\Delta(1232) \to \eta\pi^0 N$ chain, where (due to the excitation of Δ resonances) no neutron–proton cancellation can occur. Furthermore, in this reaction η mesons with small momenta relative to the target nucleus are produced, which is favorable for the formation of bound states.

2. Experimental setup

The experiments were done at the electron accelerator ELSA in Bonn [38, 39] using a 2.8 GeV electron beam. Real photons were produced by Bremsstrahlung of a copper foil (0.3 % radiation length). The photon energies were tagged via the momentum analysis of the scattered electrons by a magnetic spectrometer. The reaction products emerging from the liquid deuterium target were detected with an electromagnetic calorimeter covering almost the full solid angle. It was composed of the Crystal Barrel detector (1290 CsI crystals covering the full azimuthal angle for polar angles between 30° and 168°) [40] and the TAPS detector (528 BaF_2 crystals mounted as hexagonal forward wall covering polar angles down to 4.5°) [41, 42]. Plastic veto detectors in front of the TAPS modules and a scintillating fiber detector [43] inside the Barrel were used for charged particle identification. A schematic view of the arrangement is shown in Fig. 1, more details can be found in [27].

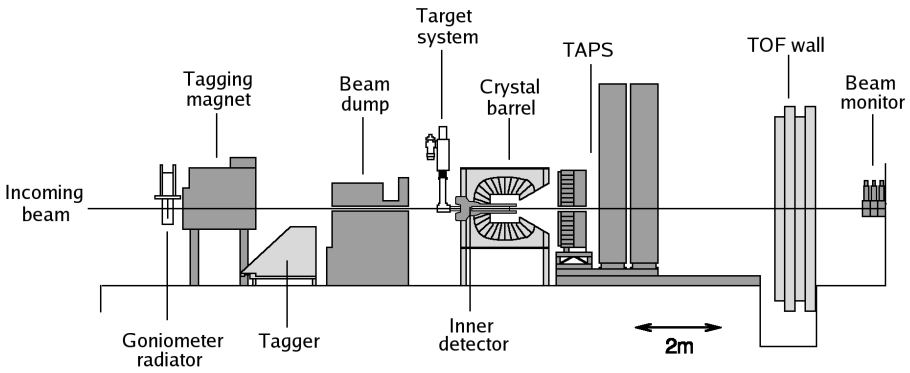

Fig. 1. Overview of the experimental setup.

3. Data analysis

The decay modes into photons were used for the identification of the neutral mesons ($\eta \to 3\pi^0 \to 6\gamma$, $\eta \to 2\gamma$, $\eta' \to \pi^0\pi^0\eta \to 6\gamma$, $\pi^0 \to 2\gamma$, $\omega \to \pi^0\gamma \to 3\gamma$). Due to trigger restrictions (see Ref. [27] for details) only channels with at least four photons were investigated, this means *e.g.* that for single η production only $\eta \to 6\gamma$ was explored, while the two-photon decay of the η was used for the $\pi^0\eta$ final state and the η' decay. Separation of photons, neutrons, protons, and charged pions in TAPS can be achieved with the charged particle veto detectors, a time-of-flight *versus* energy analysis, and a pulse-shape analysis of the BaF_2 signals (see Ref. [44] for details). The photon identification in the Crystal Barrel (see Ref. [45] for details) is

based on a cluster search algorithm and uses the information from the three layer scintillating fiber detector for rejection of charged particles. However, in this case neutrons cannot be distinguished from photons.

The analysis of the different final states is similar, as an example we will discuss quasi-free η production and give some details on the identification of the coherent production of meson pairs. For single η mesons in the first step of the analysis, events with at least six neutral PED's (Particle Energy Deposits) (see references [9, 11]) have been selected. The three invariant masses of all possible disjunct combinations of the six photons into three pairs have been calculated and only events where at least in one combination all three invariant masses passed a cut for the π^0 mass ($110< m_{\gamma,\gamma} <160$) where accepted. The two most important steps of the reaction identification — the six-photon invariant mass analysis for η identification and the missing mass analysis for the suppression of $\eta\pi$ final states — are summarized in Fig. 2. The missing mass (see Fig. 2) was calculated under the assumption of quasi-free meson production on a nucleon at rest from the incident photon energy and the energy and momentum of the η meson. For valid events it must correspond to the nucleon mass. The Fermi motion of the bound nucleons broadens the missing mass peaks, however it was still possible to separate single η production from the main background channel which is the $\eta\pi$ final state. A very conservative cut on missing mass was used, in order to avoid any contamination from this background, which rises strongly in the energy region of main interest. The background level in the invariant mass spectra after the cut on missing mass was low. It was eliminated by fitting

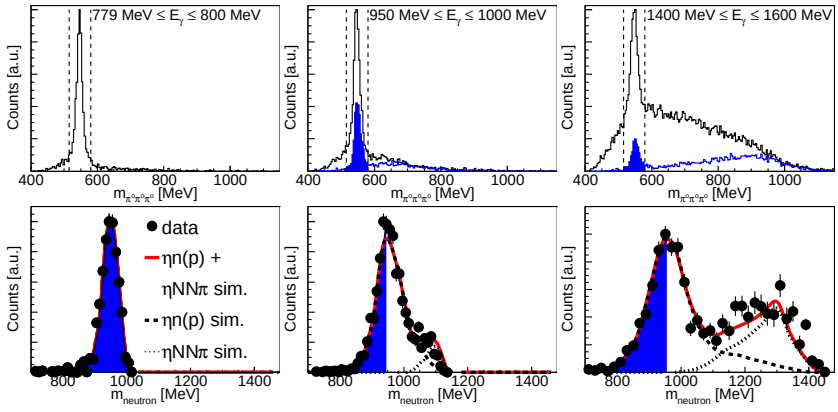

Fig. 2. Identification of $n(\gamma,\eta)n$ with invariant and missing mass analysis. Upper row: invariant mass spectra, shaded (color: blue) after cut on missing mass. Bottom row: missing mass spectra. Curves: Monte Carlo simulation of quasi-free η production, $\eta\pi$ final states and sum of both (color: red). Shaded areas (color: blue): accepted events.

the invariant mass distributions for each bin of incident photon energy and η polar angle with the peak line shape and a polynomial background.

Examples for the separation of recoil protons, neutrons, and deuterons in TAPS are shown in Figs 3 and 4. The spectra for charged recoil nucleons show clear bands for the proton and the deuteron, while the neutral hits are

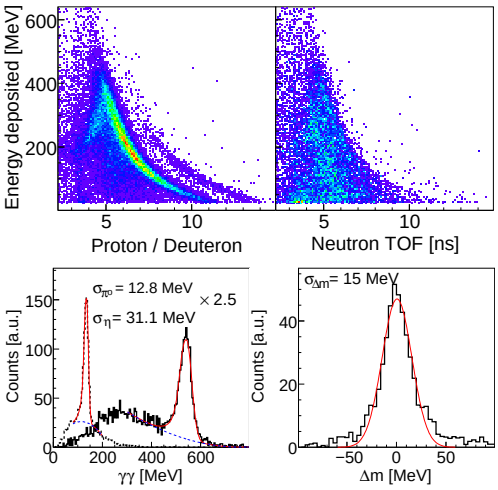

Fig. 3. Identification of $d(\gamma,\eta\pi^0)d$. Upper row: time-of-flight *versus* energy for $\eta\pi^0$ candidates with additional charged (left-hand side) and neutral (right-hand side) hits in TAPS (veto fired). Bottom row: η and π^0 invariant mass spectra and missing mass spectrum in coherent kinematics for $\eta\pi^0$ (after cut on deuteron tof-E-band).

scattered over a large area since the neutrons deposit their energy only partly in the detector. Spectra for single η production are similar, but missing the deuteron band since coherent single η production has an extremely small cross-section. Figs. 3 and 4 demonstrate also the clean identification of the $d(\gamma,\eta\pi^0)d$ and $d(\gamma,\omega\pi^0)d$ coherent reactions (spectra obtained after cut on the deuteron tof *versus* E bands). Note the narrow width of the missing mass spectra, which are not broadened by Fermi motion like the spectra from quasi-free η production in Fig. 2. Recoil protons going into the Barrel have been identified with the inner scintillating fiber detector. In the Barrel neutrons cannot be separated from photons. Therefore, for reactions with N decay photons and a further neutral hit in the Barrel first N neutral hits were assigned as decay photons via invariant mass analyses and then the left-over neutral hit was treated as recoil neutron.

The largest systematic uncertainty for the extraction of quasi-free neutron cross-sections stems from the detection efficiency of the coincident recoil neutrons. The efficiency was determined with Monte Carlo simulations,

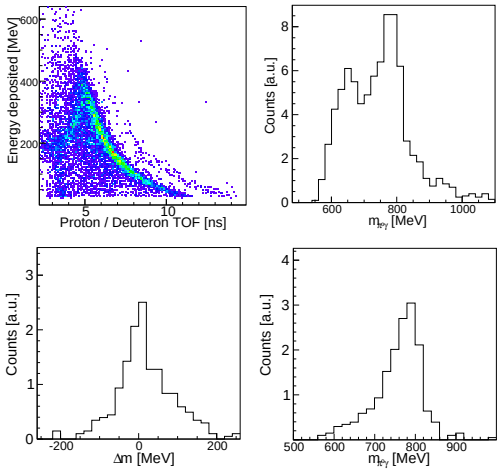

Fig. 4. Identification of $d(\gamma, \omega\pi^0)d$. Upper left corner: time-of-flight *versus* energy for charged hits in TAPS. Upper right corner: ω invariant mass for $\omega\pi^0$ candidates after cut on deuteron band. Bottom row: missing mass and ω invariant mass after cut on missing mass.

which are however, notoriously difficult for neutrons (strongly dependent on thresholds *etc.*). However, since in most cases (in particular single η, η', and $\pi^0\pi^0$ reactions) the coherent production process is completely negligible, the

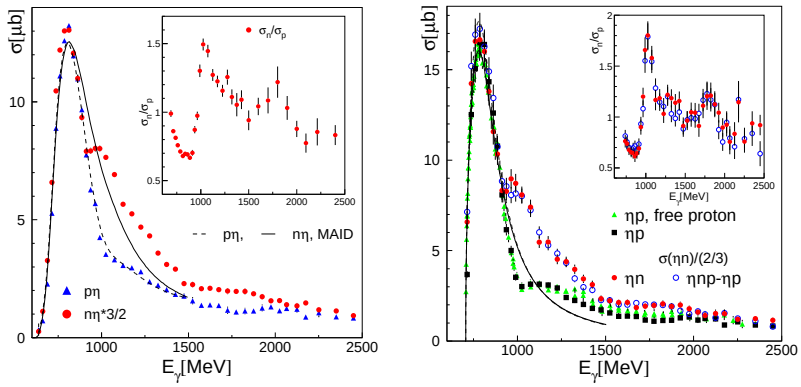

Fig. 5. Left-hand side: measured cross-sections for η photoproduction off quasi-free protons and quasi-free neutrons bound in the deuteron (neutron data normalized by factor 3/2). Insert: cross-section ratio. Curves: results of the Eta-MAID model [20] folded with momentum distributions of bound nucleons. Right-hand side: excitation functions after correction for the nucleon momentum distribution. Green triangles: free proton data, black squares: quasi-free proton data after correction for Fermi smearing. Red and blue circles: quasi-free neutron data after correction of Fermi smearing. Curves: BW-fits. Insert: cross-section ratio.

data allow for an independent test of the recoil nucleon detection efficiencies. For this purpose the $n(\gamma, x)n$ cross-sections have been determined in two different ways. In one analysis the mesons were detected in coincidence with recoil neutrons. In the other, first the inclusive cross-section without any condition for recoil nucleons was determined and then the cross-section for the reaction in coincidence with recoil protons was subtracted. The first analysis relies on the neutron detection efficiency, the second on the completely different proton detection efficiency. In all cases excellent agreement was found (see Fig. 5, right-hand side, Fig. 6, left-hand side), indicating a good control of the detection efficiencies.

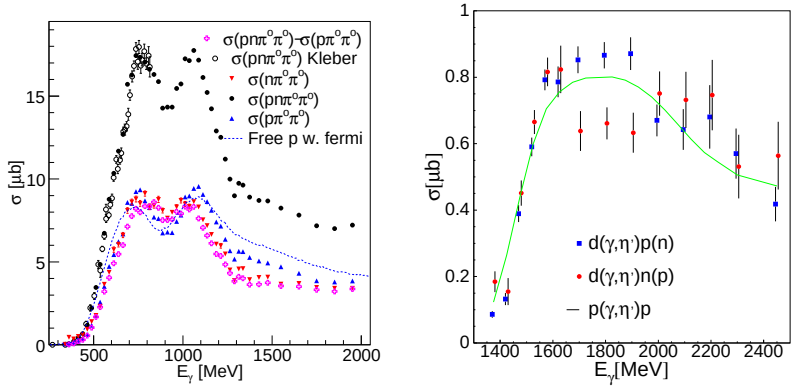

Fig. 6. Left-hand side: excitation functions for inclusive and exclusive double π^0 photoproduction. Right-hand side: comparison of quasi-free photoproduction of η' mesons of proton and neutron. All results preliminary.

4. Results

Part of the results for the single η channel have been recently published [46]. The measured total cross-sections are shown in Fig. 5 and the main findings can be summarized as follows. The results confirm the previous measurements in the $S_{11}(1535)$ resonance peak, where a neutron/proton cross-section ratio of $\approx 2/3$ is found. After normalizing the neutron data by a factor of $3/2$, the excitation functions for proton and neutron up to incident photon energies of roughly 0.9 GeV are very similar. However, at photon energies around 1 GeV a prominent structure appears in the neutron excitation function, which is not seen for the proton. So far, it was not possible to clarify the nature of this structure via model analyses of the excitation function and the angular distributions. Different scenarios involving the interference structure in the S_{11} partial wave, or resonances of different widths and quantum numbers cannot be excluded [47].

The excitation functions measured off quasi-free nucleons bound in the deuteron are smeared out by Fermi motion. An estimate of this effect was obtained in the following way. The excitation functions predicted from the MAID model [20] were folded with the nucleon momentum distributions calculated from the deuteron wave function [48]. The result is shown on the left-hand side of Fig. 5. In the proton case, almost perfect agreement indicates that the folding procedure is well under control. The agreement is not so good for the neutron, where the data shows a much sharper structure than the model. Nevertheless, in both cases we have calculated approximate correction factors from the ratio of folded and unfolded distributions and applied them to the data. The result is shown on the right-hand side of Fig. 5. The corrected quasifree proton data are compared to the free proton data. Excellent agreement is found. Below energies of 900 MeV, proton and neutron data have identical shapes. A fit in this energy range with a Breit–Wigner parameterization like in [3] reproduces the $S_{11}(1535)$ parameters extracted from photoproduction off the free proton. It yields $W = 1538\,\mathrm{MeV}$ for proton and neutron data, $\Gamma = 157$ (proton), $\Gamma = 148\,\mathrm{MeV}$ (neutron), and $A^p_{1/2} = 103$, $A^n_{1/2} = 85$ in units of $10^{-3}\mathrm{GeV}^{-1/2}$. In the cross-section ratio, the peak around 1 GeV is more pronounced and narrow than in the uncorrected data, but this is still only an upper limit for the true width of this structure. It was also attempted to correct the Fermi smearing event-by-event (see [46]) using the measured momentum vector of the recoil nucleon. This, however, is limited by the resolution of the neutron time-of-flight measurement and yielded an upper limit of the width of 60 MeV. Quasifree neutron data for further reaction channels are under analysis and will be published soon. As an example, we show in Fig. 6 preliminary excitation functions for double π^0 and η' production. In both cases again the neutron cross-sections extracted directly from the detection of recoil neutrons agree with the difference of inclusive and proton cross-sections, demonstrating the good control of systematic effects.

In the case of η' proton and neutron cross-sections differ at intermediate energies around 1.8 GeV. In this energy range also the shape of the angular distributions (not shown) is quite different. Like the η, the η' has the advantage that due to its isoscalar nature, contributions from $N^\star$ and Δ resonances can be easily disentangled: only $N^\star$'s can decay via η, η' emission to the nucleon ground state, while $\Delta^\star$'s have to decay to the $\Delta(1232)$, and thus contribute only to the $\eta\pi$, $\eta'\pi$ channels. However, so far η' production was not much explored, and the results from different analyses are contradictory. Mukhopadhyay and coworkers [49] analyzed old bubble chamber data with their effective Lagrangian model and concluded that the dominant contribution comes from the excitation of a $D_{13}(2080)$ resonance. Analyses of a more recent measurement of $p(\gamma,\eta')p$ with the SAPHIR detector [50] claimed con-

tributions from different resonances (S_{11}, P_{11}) and strong t-channel contributions. However, these results are not in good agreement with the most recent measurement by the CLAS-group [51]. An analysis of the CLAS data by Nakayama and Haberzettl [52] reveals possible contributions from S_{11}, P_{11}, P_{13}, D_{13}, and t-channel processes. The new data for the neutron target is currently under analysis in the framework of this model and is expected to help to clarify the resonance contributions.

Double pion production, in particular the $\pi^0\pi^0$ — but also the $\pi^0\pi^+$ final state, [53–64] is well suited for the investigation of nucleon resonances which decay preferentially not directly to the nucleon ground state but to other excited states. However, in spite of all the experimental efforts, so far the interpretation of the results in terms of resonance contributions is still contradictory. For the deuteron so far only the inclusive $d(\gamma,\pi^0\pi^0)X$ excitation function had been measured to incident photon energies up to 800 MeV [65]. From the present experiment precise excitation functions for $n(\gamma,\pi^0\pi^0)n$ up to 2 GeV as well as Dalitz plots of this reaction can be extracted and included in the partial wave analysis, which will put much more severe constraints on the isospin degree of freedom.

Finally, it came as a real surprise that the coherent production of meson pairs and even triplets was observed. They may lead to novel approaches for example for the search of mesic nuclei. So far, clear signals for $\eta\pi^0$, $\omega\pi^0$, $\pi^0\pi^0\pi^0$, and $\eta\pi^0\pi^0$ have been observed. Here we shortly discuss the $\eta\pi^0$-channel. The analysis of this reaction off the free proton [66, 67] has clearly identified a dominant contribution from the $\gamma p \to \Delta^\star \to \Delta(1232)\eta \to d\pi^0\eta$ reaction chain. The energy distributions of the mesons (see Fig. 7) support the dominance of $\Delta^\star \to \Delta(1232)\eta$ contributions also for the coherent reaction. For all incident photon energies, the pion kinetic energies peak at

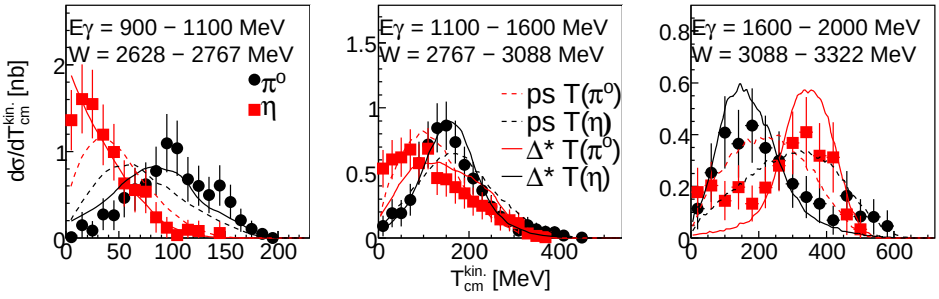

Fig. 7. Kinetic energy distributions of π^0 and η mesons from the reaction $\gamma d \to d\pi^0\eta$ for different bins of incident photon energies. Dashed curves: phase space simulations, solid curves: simulations of the $\gamma d \to d^\star(\Delta^\star) \to d^\star(\Delta(1232))\eta \to d\pi^0\eta$ reaction chain (very preliminary results).

values characteristic for $\Delta(1232) \to N\pi$ decays, while the η kinetic energies increase considerably with incident photon energy. In this way, in the threshold region, η mesons with very small kinetic energies are produced, which are an ideal tool for the study of η–nucleus interactions.

This work was supported by Schweizerischer Nationalfonds and Deutsche Forschungsgemeinschaft (SFB/TR-16).

REFERENCES

[1] V.D. Burkert, T.-S. Lee, *Int. J. Mod. Phys.* **E13**, 1035 (2004).
[2] B. Krusche, S. Schadmand, *Prog. Part. Nucl. Phys.* **51**, 399 (2003).
[3] B. Krusche *et al., Phys. Rev. Lett.* **74**, 3736 (1995).
[4] B. Krusche *et al., Phys. Lett.* **B397**, 171 (1997).
[5] J. Ajaka *et al., Phys. Rev. Lett.* **81**, 1797 (1998).
[6] A. Bock *et al.*, *Phys. Rev. Lett.* **81**, 534 (1998).
[7] F. Renard *et al., Phys. Lett.* **B528**, 215 (2002).
[8] M. Dugger *et al., Phys. Rev. Lett.* **89**, 222002 (2002).
[9] V. Crede *et al., Phys. Rev. Lett.* **94**, 012004 (2005).
[10] T. Nakabayashi *et al., Phys. Rev.* **C74**, 035202 (2006).
[11] O. Bartholomy *et al., Eur. Phys. J.* **A33**, 133 (2007).
[12] D. Elsner *et al., Eur. Phys. J.* **A33**, 147 (2007).
[13] B. Krusche *at al., Phys. Lett.* **B358**, 40 (1995).
[14] P. Hoffmann-Rothe *et al., Phys. Rev. Lett.* **78**, 4697 (1997).
[15] V. Hejny *et al., Eur. Phys. J.* **A6**, 83 (1999).
[16] J. Weiss *et al., Eur. Phys. J.* **A11**, 371 (2001).
[17] V. Hejny *et al., Eur. Phys. J.* **A13**, 493 (2002).
[18] J. Weiss *et al., Eur. Phys. J.* **A16**, 275 (2003).
[19] M. Pfeiffer *et al., Phys. Rev. Lett.* **92**, 252001 (2004).
[20] W.-T. Chiang *et al., Nucl. Phys.* **A700**, 429 (2002).
[21] W.-M. Yao *et al., J. Phys. G* **33**, 1 (2006).
[22] R.A. Arndt *et al., Phys. Rev.* **C69**, 035208 (2004).
[23] V. Kuznetsov *et al., Phys. Lett.* **B647**, 23 (2007).
[24] M. Röbig-Landau *et al., Phys. Lett.* **B373**, 45 (1996).
[25] T. Yorita *et al., Phys. Lett.* **B476**, 226 (2000).
[26] T. Kinoshita *et al., Phys. Lett.* **B639**, 429 (2006).
[27] T. Mertens *et al., Eur. Phys. J.* **A38**, 195 (2008).
[28] H. Calén *et al., Phys. Lett.* **B366**, 366 (1996).

[29] J. Smyrski *et al., Phys. Lett.* **B474**, 182 (2000).
[30] P. Moskal *et al., Phys. Rev.* **C69**, 025203 (2004).
[31] F. Plouin *et al., Phys. Rev. Lett.* **65**, 690 (1990).
[32] H. Calén *et al., Phys. Rev. Lett.* **80**, 2069 (1998).
[33] B. Mayer *et al., Phys. Rev.* **C53**, 2068 (1996).
[34] J. Smyrski *et al., Phys. Lett.* **B649**, 258 (2007).
[35] T. Mersmann *et al., Phys. Rev. Lett.* **98**, 242301 (2007).
[36] N. Willis *et al., Phys. Lett.* **B406**, 14 (1997).
[37] F. Hibou *et al.*, *Eur. Phys. J.* **A7**, 537 (2000).
[38] D. Husman, W.J. Schwille, *Phys. Bl.* **44**, 40 (1988).
[39] W. Hillert, *Eur. Phys. J.* **A28**, 139 (2006).
[40] E. Aker *et al., Nucl. Instrum. Methods* **A321**, 69 (1992).
[41] R. Novotny, *IEEE Trans. Nucl. Science* **38**, 379 (1991).
[42] A.R. Gabler *et al., Nucl. Instrum. Methods* **A346**, 168 (1994).
[43] G. Suft *et al., Nucl. Instrum. Methods* **A538**, 416 (2005).
[44] F. Bloch *et al., Eur. Phys. J.* **A32**, 219 (2007).
[45] H. van Pee *et al., Eur. Phys. J.* **A31**, 61 (2007).
[46] I. Jaegle *et al., Phys. Rev. Lett.* **100**, 252002 (2008).
[47] A.V. Anisovich *et al.*, `arXiv:0810.1849`.
[48] M. Lacombe *et al., Phys. Lett.* **B101**, 139 (1981).
[49] J.F. Zhang *et al., Phys. Rev.* **C52**, 1134 (1995).
[50] R. Plötzke *et al., Phys. Lett.* **B444**, 555 (1998).
[51] M. Dugger *et al., Phys. Lett. Rev.* **96**, 169905 (2006).
[52] K. Nakayama, H. Haberzettl, *Phys. Rev.* **C73**, 045211 (2006).
[53] F. Härter *et al., Phys. Lett.* **B401**, 229 (1997).
[54] A. Zabrodin *et al., Phys. Rev.* **C55**, R1617 (1997).
[55] A. Zabrodin *et al., Phys. Rev.* **C60**, 055201 (1999).
[56] M. Wolf *et al., Eur. Phys. J.* **A9**, 5 (2000).
[57] W. Langgärtner *et al., Phys. Rev. Lett.* **87**, 052001 (2001).
[58] Y. Assafiri *et al., Phys. Rev. Lett.* **90**, 222001 (2003).
[59] J. Ahrens *et al., Phys. Lett.* **B551**, 49 (2003).
[60] J. Ahrens *et al., Phys. Lett.* **B624**, 173 (2005).
[61] J. Ajaka *et al., Phys. Lett.* **B651**, 108 (2007).
[62] U. Thoma *et al., Phys. Lett.* **B659**, 87 (2008).
[63] A.V. Sarantsev *et al., Phys. Lett.* **B659**, 94 (2008).
[64] J. Ahrens *et al., Eur. Phys. J.* **A34**, 11 (2007).
[65] V. Kleber *et al., Eur. Phys. J.* **A9**, 1 (2000).
[66] I. Horn *et al., Phys. Rev. Lett.* **101**, 202002 (2008).
[67] I. Horn *et al., Eur. Phys. J.* **A38**, 173 (2008).